

Scaling exponents of forced polymer translocation through a nanopore

A. Bhattacharya^{1,a}, W.H. Morrison¹, K. Luo², T. Ala-Nissila^{2,3}, S.-C. Ying³, A. Milchev⁴, and K. Binder⁵

¹ Department of Physics, University of Central Florida, Orlando, FL 32816-2385, USA

² Department of Applied Physics, Helsinki University of Technology, P.O. Box 1100, FIN-02015 TKK, Espoo, Finland

³ Department of Physics, Box 1843, Brown University, Providence, RI 02912-1843, USA

⁴ Institute of Physical Chemistry, Bulgarian Academy of Sciences, Georgi Bonchev Street, Block 11, 1113 Sofia, Bulgaria

⁵ Institut für Physik, Johannes Gutenberg Universität Mainz, Staudinger Weg 7, 55099, Mainz, Germany

Received 13 February 2009 and Received in final form 2 June 2009

© EDP Sciences / Società Italiana di Fisica / Springer-Verlag 2009

Abstract. We investigate several properties of a translocating homopolymer through a thin pore driven by an external field present inside the pore only using Langevin Dynamics (LD) simulations in three dimensions (3D). Motivated by several recent theoretical and numerical studies that are apparently at odds with each other, we estimate the exponents describing the scaling with chain length (N) of the average translocation time $\langle\tau\rangle$, the average velocity of the center of mass $\langle v_{\text{CM}}\rangle$, and the effective radius of gyration $\langle R_g\rangle$ during the translocation process defined as $\langle\tau\rangle \sim N^\alpha$, $\langle v_{\text{CM}}\rangle \sim N^{-\delta}$, and $R_g \sim N^\nu$ respectively, and the exponent of the translocation coordinate (s -coordinate) as a function of the translocation time $\langle s^2(t)\rangle \sim t^\beta$. We find $\alpha = 1.36 \pm 0.01$, $\beta = 1.60 \pm 0.01$ for $\langle s^2(t)\rangle \sim \tau^\beta$ and $\bar{\beta} = 1.44 \pm 0.02$ for $\langle \Delta s^2(t)\rangle \sim \tau^{\bar{\beta}}$, $\delta = 0.81 \pm 0.04$, and $\bar{\nu} \simeq \nu = 0.59 \pm 0.01$, where ν is the equilibrium Flory exponent in 3D. Therefore, we find that $\langle\tau\rangle \sim N^{1.36}$ is consistent with the estimate of $\langle\tau\rangle \sim \langle R_g\rangle/\langle v_{\text{CM}}\rangle$. However, as observed previously in Monte Carlo (MC) calculations by Kantor and Kardar (Y. Kantor, M. Kardar, Phys. Rev. E **69**, 021806 (2004)) we also find the exponent $\alpha = 1.36 \pm 0.01 < 1 + \nu$. Further, we find that the parallel and perpendicular components of the gyration radii, where one considers the “*cis*” and “*trans*” parts of the chain separately, exhibit distinct out-of-equilibrium effects. We also discuss the dependence of the effective exponents on the pore geometry for the range of N studied here.

PACS. 87.15.A- Theory, modeling, and computer simulation – 87.15.H- Dynamics of biomolecules – 36.20.-r Macromolecules and polymer molecules

1 Introduction

Translocation of biopolymers across a biomembrane, *e.g.*, transport of RNA molecules out of a nucleus, invasion of viruses into cells, etc., are ubiquitous and important processes in biological systems [1]. Recently voltage-driven translocation of a single-stranded DNA through a α -hemolysin pore in biomembrane [2], and subsequently double-stranded DNA through synthetic silicon nanopores [3] have stimulated a lot of activities as the phenomenon is rich in fundamental science and its technical applications for detecting DNA/RNA sequences. While it is the attributes of heteropolymer translocation that are the key ingredients for prospective new sequencing methods, these experiments have generated stimulating theoretical and numerical studies directed towards fundamental physics of homopolymer translocation through a

nanopore. An important question that has been repeatedly raised is how does the average translocation time scale with the chain length? And, what is the equation of motion that describes the situation adequately? Approaches using Fokker-Planck equation with an entropic barrier term incorporated in the free energy have generated useful insights to the problem [4–12]. More recently partial Fokker-Planck equation (PFPE) has been suggested as the natural language of the problem [9,10]. Recently Sakaue [11] made an interesting prediction about the translocation exponent by viewing the process as a propagation of tensile force along the chain backbone. Quite naturally, a number of simulational studies have been directed to test predictions of these theories [7–27].

This paper is aimed at determining the relevant scaling exponents of forced translocation of a homopolymer through a nanopore by carrying out large-scale Langevin dynamics (LD) simulations in three dimensions (3D) and comparing the findings with those predicted by theoretical

^a e-mail: aniket@physics.ucf.edu

arguments. We look at the arguments for the unbiased case first as it serves as the reference for extending the theoretical arguments in the presence of an external field. Naturally, the equilibrium radius of gyration $R_g \sim N^\nu$ of a chain of length N , where ν is the equilibrium Flory exponent, is used as the relevant length scale in all the theories. The first theoretical argument came from Chuang *et al.* [7] who predicted that for the unbiased translocation the mean translocation time should scale in the same manner as a freely diffusing chain so that $\langle \tau \rangle \sim R_g^2/D \sim N^{1+2\nu}$, assuming the diffusion coefficient $D \sim 1/N$ appropriate for the free-draining limit (no hydrodynamic interaction). In this theory it is argued that the Rouse relaxation serves as the lower bound and in the presence of a nanopore a smaller amplitude accounts for the slowness of the process [15]. This theory also predicts that the scaling exponent of the reaction coordinate defined as $\langle s^2(t) \rangle \sim t^\beta$ is given by $\beta = 2/\alpha$. As usual [4–12] we denote by $s(t)$ the monomer that is inside the pore at time t . Noticeably, the theory is essentially very simple and the exponents are functions of ν only with $\alpha = 1 + 2\nu$, $\beta = 2/(1 + 2\nu)$ so that $\alpha\beta = 2$. In two dimensions (2D) $\nu = 0.75$ leads to $\alpha = 2.5$ and $\beta = 0.8$, respectively. In three dimensions (3D) $\nu = 0.588$ leads to $\alpha = 2.2$ and $\beta = 0.92$, respectively. The theory put forward by Dubbledam *et al.* invokes an additional surface exponent term γ_1 [28] so that for the diffusive case this theory predicts [9, 10] $\alpha = 2(1 + \nu) - \gamma_1$ and $\beta = 2/\alpha$. For unbiased translocation this theory also predicts the product $\alpha\beta = 2$. Several recent numerical studies in 2D [7, 16–18] and in 3D [19, 22] support Chuang *et al.*, while Dynamic Monte Carlo (DMC) results by Dubbledam *et al.* report $\alpha = 2.5$ and $\beta = 0.8$ in 3D which contradicts Chuang *et al.* and supports their own prediction [9]. While all the simulation studies verify $\alpha\beta = 2.0$, recent theories by Panja *et al.* and Vocks *et al.* pointed out the role of decay time of monomer density near the pore and argue that the translocation time is anomalous up to the Rouse time $t_R \sim N^{1+2\nu}$, and becomes diffusive afterwards [13, 14].

Let us now look at the theoretical studies of driven translocation whose numerical verification including the underlying assumptions is the main focus of the paper. According to Kantor and Kardar [8]

$$\langle \tau \rangle \sim \langle R_g \rangle / \langle v_{CM} \rangle \sim N^{1+\nu}, \quad (1)$$

assuming $\langle v_{CM} \rangle \sim 1/N$. Kantor and Kardar [8] argued that since the chain is only driven at one point inside the narrow pore, the accompanying change in its shape due to the bias is insignificant for the rest of the chain and, therefore, the chain in this case can also be described by the equilibrium Flory exponent ν . To verify their scaling argument Kantor and Kardar carried out lattice MC simulations of self-avoiding chains in 2D and noticed that the numerical exponent $\simeq 1.5 < 1 + \nu = 1.75$. They argued that finite-size effects are severe in this case and the relation $\langle \tau \rangle \sim N^{1+\nu}$ should be taken as an upper bound that will be seen only for the extremely large chains. Vocks *et al.* on the contrary, using arguments about memory effects in the monomer dynamics came up with an

alternate estimate [14] $\langle \tau \rangle \sim N^{\frac{1+2\nu}{1+\nu}}$ in 3D. Vocks argued that this estimate in 3D is superseded in 2D by a more stringent restriction of conservation of energy so that in 2D $\langle \tau \rangle \sim N^{2\nu}$. This seems to be consistent with some of the numerical data in 3D. However this estimate fails to capture the recent 2D simulation results using Langevin dynamics and MC simulations [17, 18] where one sees a crossover of the α -exponent from $1.5(2\nu)$ to $1.7(1 + \nu)$ (as opposed to 1.428). Dubbledam *et al.* have extended their PFPE-based theory for the driven translocation [10] and came up with the following relations: $\alpha = 2\nu + 1 - \gamma_1$ and $\beta = 4/(2(1 + \nu) - \gamma_1)$. The prediction of Dubbledam *et al.* for the exponents are $\alpha = 1.55$ and $\beta = 1.56$ in 2D and $\alpha = 1.5$, and $\beta = 1.6$ in 3D, respectively. The DMC results of Dubbledam *et al.* are consistent with this theory. However, numerical results using LD and MD [25, 29] produce similar results which are only in partial agreement with these theories. Sakaue [11] treated the polymer translocation problem (albeit in a slightly different context) in terms of nonequilibrium response where translocation is viewed as a propagation of a defect (defined as the confluence of relaxed and stressed parts of the chain) and comes up with the scaling exponents $\alpha = (1 + 3\nu)/2$ and $\alpha = (1 + \nu + 2\nu^2)/(1 + \nu) = 1.44$ (3D) with and without the hydrodynamic interactions, respectively. Recently a one-dimensional model has been proposed by Gauthier and Slater [26] where they studied forced polymer translocation using biased MC scheme [26] and suggested that the translocation exponent $\alpha \rightarrow 1 + \nu$ in the limit of very large chain length ($N \sim 10^6$).

In this paper not only we calculate the exponents α and β for the driven chain but provide insights how these exponents are affected by boundary and geometric factors by monitoring some of the relevant time-dependent quantities during the translocation process. This allows us to check how well some of the assumptions are satisfied for the driven translocation and discuss possible scenarios for the disagreements between the theoretical predictions and numerical studies.

2 The model

We have used the “Kremer-Grest” bead spring model to mimic a strand of DNA [30]. Excluded-volume interaction between monomers is modeled by a short-range repulsive LJ potential

$$U_{LJ}(r) = 4\varepsilon \left[\left(\frac{\sigma}{r} \right)^{12} - \left(\frac{\sigma}{r} \right)^6 \right] + \varepsilon \quad \text{for } r \leq 2^{1/6}\sigma \\ = 0 \quad \text{for } r > 2^{1/6}\sigma.$$

Here, σ is the effective diameter of a monomer, and ε is the strength of the potential. The connectivity between neighboring monomers is modeled as a Finite Extension Nonlinear Elastic (FENE) spring with

$$U_{FENE}(r) = -\frac{1}{2}kR_0^2 \ln(1 - r^2/R_0^2),$$

where r is the distance between consecutive monomers, k is the spring constant and R_0 is the maximum allowed separation between connected monomers. We use the Langevin dynamics with the equation of motion

$$\ddot{\vec{r}}_i = -\vec{\nabla}U_i - \Gamma\dot{\vec{r}}_i + \vec{W}_i(t).$$

Here Γ is the monomer friction coefficient and $\vec{W}_i(t)$ is a Gaussian white noise with zero mean at a temperature T , and satisfies the fluctuation-dissipation relation:

$$\langle \vec{W}_i(t) \cdot \vec{W}_j(t') \rangle = 6k_B T \Gamma \delta_{ij} \delta(t - t').$$

The purely repulsive wall consists of one monolayer of immobile LJ particles of diameter 1.5σ on a *triangular lattice* at the xy plane at $z = 0$. The pore is created by removing the particle at the center. Inside the pore, the polymer beads experience a constant force F and a repulsive potential from the inside wall of the pore. The reduced units of length, time and temperature are chosen to be σ , $\sigma\sqrt{\frac{m}{\epsilon}}$, and ϵ/k_B , respectively. For the spring potential we have chosen $k = 30$ and $R_{ij} = 1.5\sigma$, the friction coefficient $\Gamma = 1.0$, and the temperature is kept at $1.5/k_B$ throughout the simulation.

We carried out simulations for chain lengths N from 8–256 for two choices of the biasing force $F = 4$ and 6, respectively. Initially the first monomer of the chain is placed at the entry of the pore. Keeping the first monomer in its original position, the rest of the chain is then equilibrated for times at least an amount proportional to $N^{1+2\nu}$. The chain is then allowed to move through the pore driven by the field present inside the pore. When the last monomer exits the pore we stop the simulation and note the translocation time and then repeat the same for 5000 such trials.

3 Simulation results and their interpretation

Typical histograms for the passage time are shown in fig. 1 for $F = 6.0$. When the time axis is scaled by the mean translocation time $\langle\tau\rangle$ multiplied by the bias F and the peak of the distribution is normalized to unity, we observe (inset) a nice scaling of all the histograms on a single master curve. We also note that an excellent fit (solid lines) could be made with an expression $P(\tau) = A\tau^\lambda \exp(-\mu\tau)$ for all the plots with the peak position being given by $\tau_{\max} = \lambda/\mu$. We calculated the average translocation time from the weighted mean $\langle\tau\rangle = \int_0^{t_{\max}} \tau P(\tau) d\tau$, where t_{\max} for each distribution is chosen such that at t_{\max} the distribution $P(\tau)$ is about 0.01% of its peak value. We have checked that $\langle\tau\rangle$ calculated from the area is marginally greater than τ_{peak} obtained from $P(\tau)$. The scaling exponent α of the mean translocation time $\langle\tau\rangle \sim N^\alpha$ is extracted by plotting $\langle\tau\rangle$ as a function of N shown in fig. 2. From the observed data collapse on the same master curve we find that $\langle\tau\rangle \sim 1/F$ and $\langle\tau\rangle \sim N^{1.36}$.

The anomalous exponent β of the $s(t)$ coordinate (we denote MD time as t and translocation time as τ) is shown in fig. 3. For clarity, we have shown results for the two

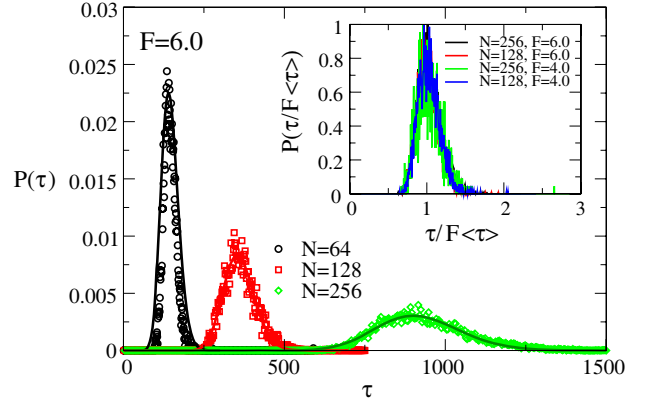


Fig. 1. Histogram $P(\tau)$ of translocation times for chain lengths $N = 64, 128,$ and 256 for bias $F = 6.0$. The symbols represent simulation data and the solid lines are fits with a form $P(\tau) = A\tau^\lambda \exp(-\mu\tau)$. The inset shows the corresponding scaled plots where the τ -axis has been scaled by $F\langle\tau\rangle$ and the y-axis has been scaled by the maximum value of the histogram.

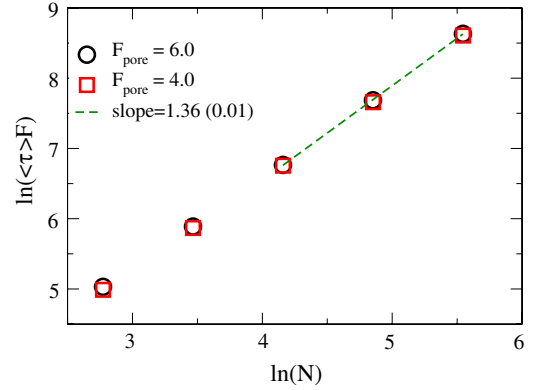


Fig. 2. Scaling of the mean translocation time $\langle\tau\rangle$ (logarithmic scale) scaled by the applied bias F as a function of chain length N (logarithmic scale). The open circles and squares refer to $F = 6.0$ and $F = 4.0$, respectively.

largest chain lengths $N = 128$ and 256 . When we calculate the first and the second moments of $s(t)$ we find that $\langle s(t) \rangle \sim t^{0.8}$ and $\langle s^2(t) \rangle \sim t^{1.6}$ for a wide range of translocation time (the slope remains the same between the blue and the green vertical windows and between the green and the red vertical windows, respectively, in fig. 3). The data as a function of the scaled translocation time Ft show excellent collapse. Since $\langle s^2(t) \rangle \sim (\langle s(t) \rangle)^2$, one expects to see $\langle \Delta s^2(t) \rangle = \langle s^2(t) \rangle - \langle s(t) \rangle^2 \sim t^{1.6}$ during the same time window. However, $\langle s^2(t) \rangle - \langle s(t) \rangle^2$ reveals additional features where the slope changes from $\langle s^2(t) \rangle - \langle s(t) \rangle^2 \sim t^{1.03}$ (between blue and green dashed vertical lines) to $\langle s^2(t) \rangle - \langle s(t) \rangle^2 \sim t^{1.44}$ (between green and red vertical lines). For the forced translocation $\langle s(t) \rangle \neq 0$ and our finding implies that the distribution function $P(s, t)$ does not have a simple scaling property where the time dependence can be absorbed via $P(s, t) = \langle s(t) \rangle^{-1} \tilde{P}(s/\langle s(t) \rangle)$, at least not for the range of time and chain length considered here. If we use the fluctuations in s to define

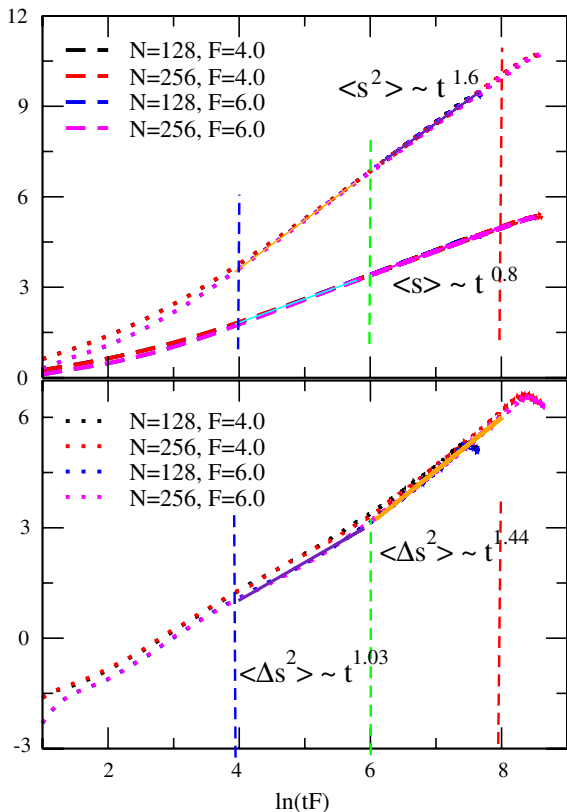


Fig. 3. (Colour on-line) Variation of $\langle s^2(t) \rangle$ (top, dotted lines) and $\langle s(t) \rangle$ (top, dashed lines), and $\langle s^2(t) - \langle s \rangle^2$ (bottom) as a function of the scaled translocation time $F\tau$. The black and blue colors correspond to a chain length $N = 128$ for $F = 4.0$ and $F = 6.0$ respectively. The red and magenta colors correspond to a chain length $N = 256$ for $F = 4.0$ and $F = 6.0$, respectively.

$\langle (s(t) - \langle s(t) \rangle)^2 \rangle \sim t^{\bar{\beta}}$, then from the late time slope (fig. 3) we get $\bar{\beta} = 1.44$.

We now compare these results with the theoretical predictions and other existing numerical results. The translocation exponent in 3D, according to Kantor and Kardar [8] is $1 + \nu = 1.588$, and according to Dubbledam [10] is 1.50. First of all, as observed in 2D MC simulations by Kantor and Kardar [8] we also obtain a smaller value of $\alpha = 1.36 \pm 0.01 < 1 + \nu = 1.588$ in 3D. Kantor and Kardar argued that a lower value is obtained due to finite size effects and expect that for very large chains one would find $1 + \nu \simeq 1.59$. This bound has recently been criticized by Vocks *et al.* [14] who, using arguments about memory effects in the monomer dynamics, came up with an alternate exponent estimate given by $\alpha = \frac{1+2\nu}{1+\nu} = 1.37$. For the pore diameter considered here our result is compatible with this prediction. However, we will come back to this issue later. As for the exponent β , we find $\langle s^2(t) \rangle \sim t^{1.6}$, and $\langle \Delta s^2(t) \rangle = \langle s^2(t) - \langle s \rangle^2 \rangle \sim t^{1.44}$ (if we use the later window). Therefore, we do not agree with Dubbledam *et al.* with the calculated value of α , but we find $\beta = 1.6$ which is exactly the same as found by Dubbledam *et al.* It is noteworthy that the fluctuation $\langle \Delta s^2(t) \rangle$ has a different time dependence and the slope of $\langle \Delta s^2(t) \rangle \sim t^{1.03}$

at early time crosses over to $\langle \Delta s^2(t) \rangle \sim t^{1.44}$ at a later time, while the slope for $\langle s^2(t) \rangle \sim t^{1.6}$ is constant for a wider range. If we use $\beta = 1.44$, obtained from the definition of fluctuation of the s coordinate, then we find that the relation $\alpha\beta = 2.0$ is satisfied for the forced translocation as well. This trend is qualitatively the same for the simulation using a square pore [29], where we find that $\langle \tau \rangle \sim N^{1.41}$, $\langle s^2(t) \rangle \sim t^{1.52}$, and $\langle \Delta s^2(t) \rangle \sim t^{1.45}$ (so that $\alpha\beta \simeq 2.0$, same as reported here if we extract β from the slope of the plot $\langle \Delta s^2(t) \rangle \sim t$). Our results may be relevant in the context of a recent article by Chatelain, Kantor, and Kardar [31] who showed that the variance of the probability distribution $P(s, t)$ grows subdiffusively.

We now look more closely at the factors responsible for the translocation process. The expression $\tau \sim \langle R_g \rangle / \langle v_{\text{CM}} \rangle \sim N^{1+\nu}$ has two components: the dependence of v_{CM} on N and R_g on N , respectively. We now look at these two components separately. During the driven translocation the chain does not find enough time to relax. Therefore, it is important to know how the shape of the chain varies as a function of time and how different it is compared to its equilibrium configuration. During the forced translocation at any instant of time only one segment of the entire chain feels the bias. Kantor and Kardar [8] argued that the shape of the chain is hardly affected by it so that it will still be described by the equilibrium Flory exponent ν . This argument will not be strictly valid for the model used here as the beads are connected by elastic bonds and it is expected that quite a few neighbors on either side of the driven bead inside the pore will be indirectly affected by it.

In order to verify this issue first, we have calculated the equilibrium $\langle R_g^{\text{eq}} \rangle$ of the chain clamped at one end at the pore in the presence of the same LJ wall. We find $\nu \sim 0.6 \pm 0.01$ (fig. 4(b)). We have also calculated the relaxation time τ_r of the end-to-end vector $\langle (\mathbf{R}_{1N}(t + \tau) - \langle \mathbf{R} \rangle) \cdot (\mathbf{R}_{1N}(t + \tau) - \langle \mathbf{R} \rangle) \rangle \sim \exp(-t/\tau_r)$ and checked that we get the same ν from the relaxation measurements ($\tau_r \sim N^{1+2\nu}$). This is consistent with the theoretical prediction of Eisenriegler, Kremer, and Binder that in the presence of the wall the exponent ν remains the same as that of its bulk counterpart [32]. To get an idea how fast is the translocation process, compared to the corresponding relaxation time, for the chain lengths $N = 64$, 128, and 256, we find $\tau_r \sim 1000$, 4500, and 20200, respectively, and the corresponding average translocation times $\langle \tau \rangle$ are 215, 530, and 1330, respectively. Even for small bias where $\langle \tau \rangle \sim 1/F$, we observe $\tau_r \gg \langle \tau \rangle$. Figure 4(a) shows the time dependence of $R_g(t)$ and its transverse and longitudinal components $R_{gt}(t)$ and $R_{gl}(t)$ averaged over both *cis* and *trans* side for chain length $N = 128$. We notice that during the translocation process, contrary to what is assumed by Kantor and Kardar, the chain is significantly elongated around $t \simeq 0.5\langle \tau \rangle$ and acquires relatively compact structure immediately upon exiting the pore. Further, the transverse component of the radius of gyration of the chain that has just translocated is distinctly smaller compared to its value at $t = 0$ (fig. 4(a)) and hence such translocated chains are not in equilibrium configurations. The dashed lines show the corresponding

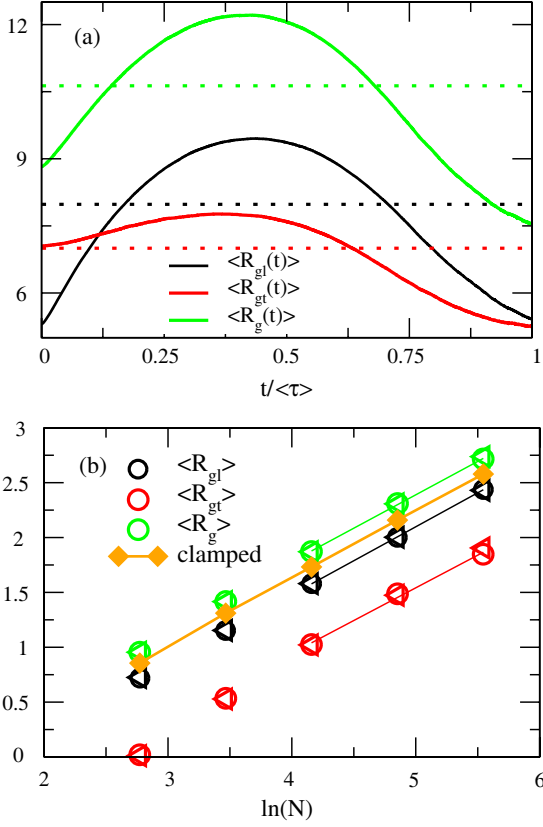


Fig. 4. (Colour on-line) (a) Plot $\langle R_{gt}(t) \rangle$, $\langle R_{gl}(t) \rangle$ and $\langle R_g(t) \rangle$ as a function of $\langle \tau \rangle$ for chain length $N = 128$. Corresponding dotted lines represent the average value. (b) Scaling of $\langle R_{gl} \rangle$ (black), $\langle R_{gt} \rangle$ (red), and $\langle R_g \rangle$ (green) as a function of chain length N . The circles and squares correspond to the applied bias $F = 6.0$ and $F = 4.0$, respectively. Orange squares correspond to the equilibrium radius of gyration R_g^{eq} for a chain clamped at the pore.

average values from which we extract the exponent $\bar{\nu} \simeq \nu$ (fig. 4(b)). Since the average linear dimensions are *dominated* by the *larger* equilibrium values at the beginning of the process, it is no surprise that we find that $\langle R_g \rangle$ scales almost the same way as $\langle R_g^{\text{eq}} \rangle \sim N^{0.6}$ (slopes are almost the same in fig. 4(b)) even when $\langle \tau \rangle \ll \tau_r$. Therefore, the chain is still described by the equilibrium $\langle R_g^{\text{eq}} \rangle$.

We have further extended the analysis by looking at the longitudinal and transverse components of the radius of gyration both on the *trans* side ($R_{gt}^{\text{trans}}(m)$ and $R_{gl}^{\text{trans}}(m)$) and *cis* side ($R_{gt}^{\text{cis}}(N-m)$ and $R_{gl}^{\text{cis}}(N-m)$), respectively, as a function of the translocated segments m . This is shown in fig. 5. One immediately notices that the $R_g(m)$ of the chain on the *cis* and *trans* side is described by different effective Flory exponents. The effect is most pronounced for the longitudinal component. We have calculated the slopes for $N/8 < m < N/4$ and find that $\langle R_{gt}^{\text{trans}}(m) \rangle \sim m^{0.6}$ and $\langle R_{gl}^{\text{cis}}(m) \rangle \sim m^{0.8}$. This result is consistent with the recent theory proposed by Sakaue [11] based on the propagation of tension along the chain. During the forced translocation process at early time ($m \ll N$) the translocated monomers relax faster

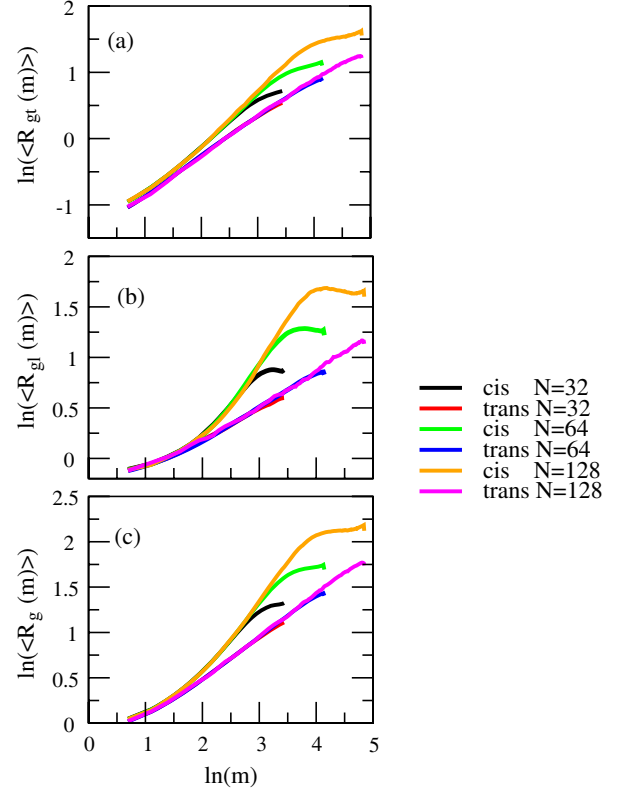


Fig. 5. (Colour on-line) Plot of (log-scale) (a) $\langle R_{gt}^{\text{cis}}(m) \rangle$, $\langle R_{gt}^{\text{trans}}(m) \rangle$, (b) $\langle R_{gl}^{\text{cis}}(m) \rangle$, $\langle R_{gl}^{\text{trans}}(m) \rangle$, and (c) $\langle R_g^{\text{cis}}(m) \rangle$, $\langle R_g^{\text{trans}}(m) \rangle$ as a function of the segments m on the *cis* and *trans* sides, respectively. In each panel black ($N = 32$), green ($N = 64$), and orange ($N = 128$) colors correspond to the *cis* segments, and red ($N = 32$), blue ($N = 64$), and magenta ($N = 128$) correspond to *trans* segments, respectively.

and are described roughly by the equilibrium Flory exponent. However, during the short time needed for a small number of m monomers to be pulled through the pore by the force, the remaining $N - m$ segments do not have enough time to equilibrate their configuration. One can think of this effect as the shape of $R_g^{\text{cis}}(N - m)$ remaining the *same* as $R_g^{\text{cis}}(N)$ but with a few *less* number of monomers that have translocated. This makes the effective Flory exponent higher on the *cis* side at the early stage of the translocation process. As time proceeds the number of monomer on the *cis* side also decreases causing the slope (fig. 5) also to decrease. This difference in behavior of $R_{gt}^{\text{trans}}(m)$ and $R_{gt}^{\text{cis}}(m)$ as manifested in our simulation studies should serve as useful information for theoretical studies of polymer translocation through a nanopore.

In order to compare with the proposal of Kantor and Kardar [8] (eq. (1)) we have monitored $\langle V_{\text{CM}}^z \rangle$. In general $\langle V_{\text{CM}}^z(t) \rangle$ will be a function of time and one may wonder how to interpret the quantity $\langle v_{\text{CM}} \rangle$ in eq. (1). In fig. 6(a) we have shown $\langle V_{\text{CM}}^z(t) \rangle \sim t$ for two different chain lengths $N = 128$ and $N = 256$, respectively. Since we are carrying out Langevin Dynamics simulation, the velocity saturates quite quickly and $F_{\text{CM}}^z = \gamma V_{\text{CM}}^z$. Since $\gamma = 1$ in our simulation we check that $\langle F_{\text{CM}}^z \rangle = \langle V_{\text{CM}}^z \rangle$ by plotting

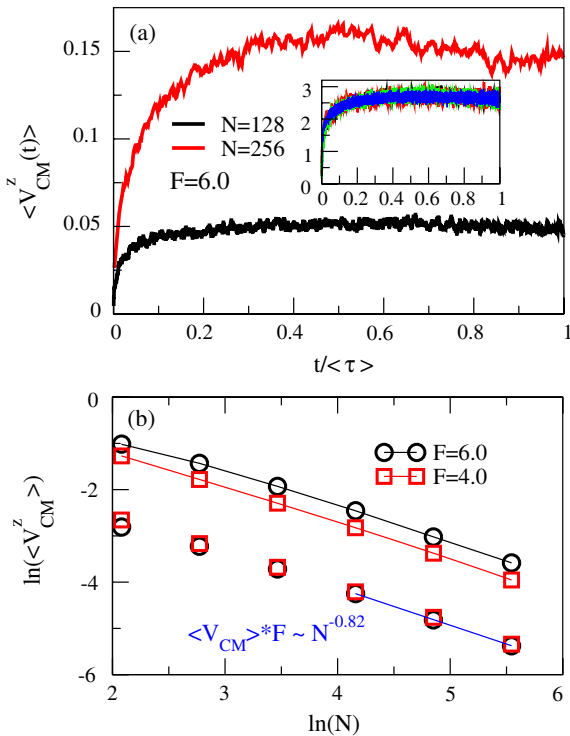


Fig. 6. (Colour on-line) (a) Plot of $\langle V_{CM}^z(t) \rangle$ for chain lengths $N = 128$ and $N = 256$, respectively. The inset shows the same where $\langle V_{CM}^z(t) \rangle$ is scaled by $N^{-0.82}$ obtained from (b) and $\langle F_{CM}^z(t) \rangle / N^{-0.82}$ (green and blue) obtained independently from simulation. (b) Scaling plot (log-scale) of $\langle V_{CM}^z \rangle$ as a function of chain length N .

$F_{CM}^z(t)$ independently calculated from simulation. The inset of fig. 6(a) shows the plots for $\langle V_{CM}^z(t) / N^{-0.82} \rangle$ and $\langle F_{CM}^z(t) / N^{-0.82} \rangle$ for chain lengths $N = 128$ and $N = 256$, where we observe excellent data collapse. This saturation value at the plateau is used as $\langle V_{CM}^z \rangle$ to calculate the dependence of $\langle V_{CM}^z \rangle$ on the chain length N shown in fig. 6(b). We also notice from the excellent data collapse that, for a small value of the bias, the relation $\langle V_{CM}^z \rangle \sim 1/F_{ext}$ holds. Since $\bar{v} \simeq \nu$, our studies indicate that it is the velocity (which does not exhibit inverse linear dependence on the chain length N) the responsible factor for the deviation from $\langle \tau \rangle \sim N^{1+\nu}$.

It is worth mentioning that we have carried out exactly the same LD simulations with wall particles on a square lattice [29]. We find that $\langle \tau \rangle \sim N^{1.41}$, $\langle s^2(t) \rangle \sim t^{1.52}$, and $\langle \Delta s^2(t) \rangle \sim t^{1.45}$ (so that $\alpha\beta \simeq 2.0$, same as reported here if we extract β from the slope of the plot $\langle \Delta s^2(t) \rangle \sim \tau$). These results for the square pore are also consistent with recently reported LD and MD simulation results in 3D using GROMACS [25]. Recently Gauthier *et al.* [22, 23] carried out similar studies of polymer translocation through a narrow pore (including hydrodynamic (HD) interactions) and found a systematic variation of the measured scaling exponents as a function of the pore width. However, their studies are limited to a relatively narrow range of N up to 31 only. In a more recent study using stochastic rotational dynamics Lehtola [27] observed that translocation

becomes faster in the presence of HD interactions but the translocation exponent is relatively insensitive to the applied bias. In our studies the exponents for a relatively wide range of N seem to depend on the pore geometry. Whether this implies true nonuniversality or not remains an open issue.

4 Conclusion

To summarize, we have used Langevin dynamics in 3D to study the scaling properties of a driven translocating chain through a nanopore. We notice that the chain undergoes a significant shape change during the fast translocation process, contrary to what assumed by Kantor and Kardar formulating the theory of forced translocation. However, despite significant distortion, a careful observation reveals that the average $\langle R_g \rangle$ is still dominated by its equilibrium value at the beginning of the translocation process and hence the chain is still described by the equilibrium Flory exponent. We find that the average velocity of the translocating chain does not scale as its bulk counterpart and depends on pore width and geometry. It is likely that density variation on either side of the pore during the translocation process affects the overall motion of the chain. We find that $\alpha = 1.36 < 1 + \nu$. It is worth mentioning that for the forced translocation collective numerical work by various groups failed to validate the Kantor and Kardar result $\alpha = 1 + \nu$. Numerical results that are obtained using a bead-spring type of model are probably dominated by out-of-equilibrium effects and the observed translocation exponents fall within the limit $2\nu < \alpha < 1 + \nu$, including the results listed here. It is likely that in the limit of small force and very large friction, where out-of-equilibrium effects will be most likely less severe, one can get a larger translocation exponent $\alpha \rightarrow 1 + \nu$ [33]. Likewise, although the value of $\alpha = 1.36$ that we obtain is consistent with the analytical estimate of Vocks *et al.* $\alpha = \frac{1+2\nu}{1+\nu} = 1.37$ in 3D [14], this result implies that the diffusion coefficient D scales as $D \sim N^{-\nu}$ [35], a result which should be true only in the presence of hydrodynamics interaction that is absent in the model of Vocks *et al.* We also note that the results from 2D simulations do not agree with the estimate of Vocks *et al.* Further, our preliminary results indicate that the α -exponent depends systematically on the pore diameter [34]. Therefore our agreement with Vocks *et al.* is fortuitous. Finally, we notice a difference in the s -exponent β when calculated from its second moment ($\beta = 1.6$) and its fluctuations ($\bar{\beta} = 1.44$). The latter value ($\bar{\beta} = 1.44$) agrees with $\alpha\bar{\beta} \simeq 2.0$, while $\beta = 1.6$ overestimates it ($\alpha\beta \simeq 2.2 > 2.0$). The fluctuations $\langle \Delta s^2(t) \rangle$ seem to reveal a more complicated time dependence not adequately studied so far.

While our results (fig. 5) for the anomalous behavior of the gyration radii of the “*cis*” part of the translocating chain is (at least qualitatively) in accord with Sakaue’s theory, the latter does not describe the “*trans*” part (this theory may be more appropriate for describing translocation of a chain that is always pulled at one of its end).

The time dependence of the radius of gyration and all its components during the translocation process (fig. 4(a) and fig. 5) is clearly a relevant feature of the translocation process and the chain configurations are out of equilibrium. Thus it seems to us questionable if simpler theories that reduce the translocation process to kinetics of the translocation reaction coordinate $s(t)$ can be accurate. Our results on the fluctuation of the translocation coordinate cast doubt on whether simple scaling descriptions work (at least for the considered range of moderate chain lengths). We have demonstrated that the translocation dynamics is characterized by out-of-equilibrium chain configurations. On the contrary “local equilibrium” hypothesis is one of the key assumptions of many existing theories. Currently we are investigating the consequences of this “local equilibrium” hypothesis which we will report in separate publication [29]. Certainly more numerical and analytic work is needed for a more comprehensive understanding of forced translocation through a nanopore.

A.B. gratefully acknowledges the local hospitality of the Institut für Physik, Johannes-Gutenberg Universität, Mainz, the travel support from the Deutsche Forschungsgemeinschaft, SFB 625/A3, and the local hospitality and travel support from the COMP Center of Excellence, Helsinki University of Technology, respectively, and thanks Prof. M. Muthukumar for valuable discussions. T.A-N. and K.L. have been in part supported by the Academy of Finland through the COMP Center of Excellence program and TransPoly consortium grant.

References

1. B. Alberts *et al.*, *Molecular Biology of the Cell* (Garland Publishing, New York, 1994).
2. J.J. Kasianowitch, E. Brandin, D. Branton, D. Deamer, Proc. Natl. Acad. Sci. U.S.A. **93**, 13770 (1996); A. Meller, L. Nivon, E. Brandin, J. Golovchenko, D. Branton, Proc. Natl. Acad. Sci. U.S.A. **97**, 1097 (2000).
3. J.L. Li, M. Gershow, D. Stein, E. Brandin, J.A. Golovchenko, Nat. Mater. **2**, 611 (2003); A.J. Storm, J.H. Chen, X.S. Ling, H.W. Zandbergen, C. Dekker, Nat. Mater. **2**, 537 (2003).
4. W. Sung, P.J. Park, Phys. Rev. Lett. **77**, 783 (1996).
5. M. Muthukumar, J. Chem. Phys. **111**, 10371 (1999).
6. D.K. Lubensky, D. Nelson, Biophys. J. **77**, 1824 (1999).
7. J. Chuang, Y. Kantor, M. Kardar, Phys. Rev. E **65**, 011802 (2001).
8. Y. Kantor, M. Kardar, Phys. Rev. E **69**, 021806 (2004).
9. J.L.A. Dubbledam, A. Milchev, V.G. Rostiashvili, T. Vilgis, Phys. Rev. E **76**, 010801(R) (2007).
10. J.L.A. Dubbledam, A. Milchev, V.G. Rostiashvili, T. Vilgis, EPL **79**, 18002 (2007).
11. T. Sakaue, Phys. Rev. E **76**, 021803 (2007).
12. J.K. Wolterink, G.T. Barkema, D. Panja, Phys. Rev. Lett. **96**, 208301 (2006).
13. D. Panja, G.T. Barkema, R.C. Ball, J. Phys.: Condens. Matter **19**, 432202 (2007); J. Phys.: Condens. Matter **20**, 075101 (2008).
14. H. Vocks, D. Panja, G.T. Barkema, R.C. Ball, J. Phys.: Condens. Matter **20**, 095224 (2008).
15. A. Milchev, K. Binder, A. Bhattacharya, J. Chem. Phys. **121**, 6042 (2004).
16. K. Luo, T. Ala-Nissila, S.-C. Ying, J. Chem. Phys. **124**, 034714 (2006).
17. K. Luo, T. Ala-Nissila, S.-C. Ying, J. Chem. Phys. **124**, 114704 (2006).
18. I. Huopaniemi, K. Luo, T. Ala-Nissila, S.-C. Ying, J. Chem. Phys. **125**, 124901 (2006).
19. D. Wei, W. Yang, X. Jin, Q. Liao, J. Chem. Phys. **126**, 204901 (2007).
20. K. Luo, T. Ala-Nissila, S.-C. Ying, A. Bhattacharya, J. Chem. Phys. **126**, 145101 (2006); Phys. Rev. Lett. **99**, 148102 (2007); **100**, 058101 (2008).
21. S. Matysiak, A. Montesi, M. Pasquali, A. Kolomeisky, C. Clementi, Phys. Rev. Lett. **96**, 118103 (2006).
22. S. Guillouzie, G.W. Slater, Phys. Lett. A **359**, 261 (2006).
23. M.G. Gauthier, G.W. Slater, Eur. Phys. J. E **25**, 17 (2008).
24. M.G. Gauthier, G.W. Slater, Phys. Rev. E **79**, 021803 (2009).
25. K. Luo, S. Ollila, I. Huopaniemi, T. Ala-Nissila, P. Pommorski, M. Karttunen, S.-C. Ying, A. Bhattacharya, Phys. Rev. E **78**, 050901(R) (2008).
26. M.G. Gauthier, G.W. Slater, J. Chem. Phys. **128**, 065103; 205103 (2008).
27. V.V. Lehtola, R.P. Linna, K. Kaski, EPL **85**, 58006 (2009); Phys. Rev. E **78**, 061803 (2008).
28. R. Hegger, P. Grassberger, J. Phys. A **27**, 4069 (1994); M.N. Barber, J. Phys. A **11**, 1833 (1978).
29. A. Bhattacharya, unpublished. Here the wall consists of a monolayer of LJ particles of $\sigma = 1$ arranged on a square lattice and the pore is created by removing 4 particles around the center.
30. G.S. Grest, K. Kremer, Phys. Rev. A **33**, 3628 (1986).
31. C. Chatelain, Y. Kantor, M. Kardar, Phys. Rev. E **78**, 021129 (2008).
32. E. Eisenriegler, K. Kremer, K. Binder, J. Chem. Phys. **77**, 6296 (1982); P.G. de Gennes, Macromolecules **13**, 1069 (1980).
33. K. Luo *et al.*, unpublished.
34. A. Bhattacharya, K. Binder, T. Ala-Nissila, unpublished.
35. J.L.A. Dubbledam, A. Milchev, V. Rostiashvili, T.A. Vilgis, J. Phys.: Condens. Matter **21**, 098001 (2009).